Quantum-classical correspondence in energy space: Two interacting spin particles

F. Borgonovi,[1,2,3] I. Guarneri,[2,3,4] and F. M. Izrailev[4,5,6]
[1]*Dipartimento di Matematica, Università Cattolica, via Trieste 17, 25121 Brescia, Italy*
[2]*Istituto Nazionale di Fisica Nucleare, Sezione di Pavia, via Bassi 6, 27100 Pavia, Italy*
[3]*Istituto Nazionale di Fisica della Materia, Unità di Milano, via Celoria 16, 22100 Milano, Italy*
[4] *Universitá di Milano, sede di Como, via Lucini 3, 22100 Como, Italy*
[5]*Budker Institute of Nuclear Physics, 630090 Novosibirsk, Russia*
[6]*Instituto de Fisica, Universidad Autonoma de Puebla, Apartado Postal J-48, Puebla 72570, Mexico*
(Received 16 December 1997)

The Hamiltonian conservative system of two interacting particles has been considered both in classical and quantum description. The quantum model has been realized using a symmetrized two-particle basis reordered in the unperturbed energy. The main attention is paid to the structure of chaotic eigenfunctions (EF's) and to the local spectral density of states (LDOS). A remarkable correspondence has been found for the shapes of EF's and the LDOS in the energy representation to their classical counterparts. Comparison with the band random matrix theory predictions has revealed quite significant differences, which are due to the dynamical nature of the model. On the other hand, a partial agreement is found by inserting randomness *ad hoc* in the dynamical model for two-body matrix elements. This shows that, at least for small number of particles, care must be taken when classical correlations are neglected. The question of quantum localization in the energy space is discussed for both the dynamical and random models. [S1063-651X(98)05005-3]

PACS number(s): 05.45.+b

I. INTRODUCTION

Quantization of classically chaotic systems has been addressed, from the very beginning, to both conservative and time-dependent systems. In the latter case the important phenomenon of dynamical localization was discovered, connecting a classical quantity, the diffusion rate, to the quantum localization length of the correspondent equilibrium distribution [1]. Instead, in the case of conservative systems, important steps have been taken in establishing some distinctive features that mark a quantum chaotic system from an integrable one: let us mention, for instance, the non-Wigner-Dyson statistics of neighboring level spacings, or the scarring of eigenfunctions along some classical periodic orbits. However, the possibility of quantum localization effects in such systems has been scarcely explored until recently, when a clue in this direction was found [2] by investigating a particular class of random models: the Wigner banded random matrices (WBRM) ensemble.

For such an ensemble, whose introduction dates back to Wigner himself [3], it is possible to obtain a series of results that allow for a definition of quantum localization within the classical energy surface. These results, when extended to Hamiltonian systems, would impose severe quantum limitations on the behavior of classical ergodic systems. The important result is that room is left for quantum localization and this can be obtained directly from the knowledge of the local spectral density of states (LDOS) and eigenfunctions (EF's). Quite surprisingly, both quantities have well-defined classical limits (see Ref. [2]) that, generally speaking, have received scarce attention before now.

On the other hand, in order to acquire physical relevance, it is clear that such results should be extended to real physical systems, where the origin of randomness is purely dynamical. This we do, in this paper, by considering a classically chaotic two-interacting spin system with a finite Hilbert space. Our purpose is analyzing the structure of eigenstates and of the LDOS, and comparing it with expectations based on previous random matrix studies and with their classical counterparts.

First of all we find that, when written in the eigenbasis of two noninteracting particles, reordered in the unperturbed energy, the Hamiltonian matrix has an overall banded structure. About the shape of eigenfunctions and the LDOS, we find that our quantum results, on the average, follow the behavior of similar quantities computed from WBRM only approximately at best. Nevertheless, they follow remarkably well the behavior of their classical analogs that we actually compute in the present paper.

On the other hand, the correspondence with random matrix theories (RMT's) is restored on artificially randomizing our Hamiltonian. The lesson we draw from this result is that, although RMT quite well reproduces fluctuation properties of spectra of real chaotic Hamiltonians, some correlations are missing in their structure, which are essential in giving the correct semiclassical behavior when detailed questions about the structure of eigenfunctions are asked. It is of course possible that a better correspondence with RMT will be restored with systems with a larger number of particles; for the time being, however, our results appear to indicate that caution is needed in carrying over results from RMT to Hamiltonians that have a smooth, well-defined classical limit.

II. MODEL

The model has been proposed and widely investigated in [4]. Here we review few fundamental facts about its classical and quantum behavior. It describes two coupled rotators, with angular momentum $\vec{L}$ and $\vec{M}$ with the following Hamiltonian:

$$H=A(L_z+M_z)+BL_xM_x. \tag{1}$$

It may be used to describe the interaction of quasispins in nuclear physics or pseudospins in solid-state systems. Choosing A^{-1} as the unit of time and AB^{-1} as the unit of angular momentum, it can be written as $H=H_0+V$ where $H_0=L_z+M_z$ and $V=L_xM_x$. The constants of motion are $H=E$, L^2, and M^2.

Fixing the values of L^2 and M^2 it can also be shown [4] that the total energy must be bounded:

$$E^2\leqslant E^2_{\max}=(L^2+1)(M^2+1) \tag{2}$$

for $LM>1$.

It is worth mentioning that in this form the dynamical variables $\vec{L},\vec{M}$ are not canonical. On the other hand, the usual Hamiltonian form, with the canonical variables q_i,p_i, $i=1,2$ can be recovered by means of the following transformation:

$$L_x=\sqrt{L^2-p_1^2}\cos q_1,\quad L_y=\sqrt{L^2-p_1^2}\sin q_1,$$
$$L_z=p_1,\quad M_x=\sqrt{M^2-p_2^2}\cos q_2,$$
$$M_y=\sqrt{M^2-p_2^2}\sin q_2,\quad M_z=p_2, \tag{3}$$

keeping L^2 and M^2 as constants [5]. In these variables the Hamiltonian reads

$$H=p_1+p_2+\sqrt{L^2-p_1^2}\sqrt{M^2-p_2^2}\cos q_1\cos q_2. \tag{4}$$

The analysis of the surfaces of section reveals a large number of regular trajectories covering invariant tori when L^2,M^2 are both very small or very large [4]. To simplify the problem we set $L=M$. In such a case the most interesting situation occurs when $1<L<10$ where, depending on the energy value E, regular and chaotic regions coexist. Typically when $|E|$ is close to $E_{\max}=L^2+1$ trajectories are regular while for $E\simeq 0$ islands of stability become very small and chaotic motion dominates.

Quantization follows standard rules, and angular momenta are quantized according to the relations $L^2=M^2=\hbar^2 l(l+1)$ where l is an integer number. Therefore, for given l the Hamiltonian is a finite matrix, and the semiclassical limit is recovered in the limit $l\to\infty$ and $\hbar\to 0$ keeping L^2 constant.

In our approach the Hamiltonian is represented in the two-particles basis $|l_z,m_z\rangle$ where the matrix elements have the form

$$\langle l_z',m_z'|H_0|l_z,m_z\rangle=\delta_{m_z,m_z'}\delta_{l_z,l_z'}\hbar(l_z+m_z) \tag{5}$$

and

$$\langle l_z',m_z'|V|l_z,m_z\rangle=\frac{\hbar^2}{4}\delta_{m_z,m_z'\pm 1}\delta_{l_z,l_z'\pm 1}\sqrt{(l+l_z)(l-l_z+1)(m+m_z)(m-m_z+1)} \tag{6}$$

with l_z,m_z integers, $-l\leqslant l_z,m_z\leqslant l$.

The z component of the total angular momentum $J_z=L_z+M_z$ (which is the same as the unperturbed Hamiltonian H_0) obeys the selection rules $\Delta J_z=0,\pm 2\hbar$, so the subspace spanned by the states with odd $J_z/\hbar$ can be separated from that with $J_z/\hbar$ even (there are no matrix elements for the transition between them). In what follows, we fix $J_z/\hbar=H_0/\hbar$ even. As a result, the matrix describing the Hamiltonian has a dimension $N=2l^2+2l+1$. We have also to take into account the symmetry degeneracy with respect to the exchange of particles. Below, we consider only symmetric states.

Let us now explain how the Hamiltonian matrix is constructed. Once l is fixed, there are $2l+1$ single-particle levels $\langle -l|,\langle -l+1|,\ldots,\langle -1|,\langle 0|,\langle 1|,\ldots,\langle l-1|,\langle l|$. The ground state is represented by two particles in the lowest single-particle level, which we label as $\langle -l,-l|$; it has an unperturbed energy $E_0=-2l\hbar$. The first excited state is doubly degenerate and the two eigenstates having the same energy $E_1=(-2l+2)\hbar$ are $(\langle -l,-l+2|+\langle -l+2,-l|)/\sqrt{2}$ and $\langle -l+1,-l+1|$. The former state corresponds to one particle in the single-particle level $\langle -l+2|$ and the other in the single-particle ground state $\langle -l|$. The latter state, to two particles in the single-particle level $\langle -l+1|$. We call the H_0 shell the set of states having the same value of unperturbed energy.

It is easy to prove that in the symmetrized basis each shell with H_0 fixed and even has a degeneracy $p=l+1-|H_0|/2\hbar$, and the dimension of the Hamiltonian matrix is $N=(l+1)^2$ due to the relation

$$\sum_{H_0/2=-\hbar l}^{\hbar l}\left(l+1-\frac{|H_0|}{2\hbar}\right)=(l+1)^2.$$

We then reorder the Hamiltonian matrix according to the increasing unperturbed energies and we call $|\mathbf{n}\rangle$ the resulting two-particles symmetrized ordered basis. As a result, the off-diagonal matrix elements are symmetric with respect to the two main diagonals $H_{n,n}=\langle\mathbf{n}|H|\mathbf{n}\rangle$ and $H_{N-n,N-n}$.

Diagonal matrix elements are constructed from the unperturbed Hamiltonian H_0; they are given by the eigenvalues $-2l\hbar,(-2l+2)\hbar,\ldots,2l\hbar$ and are disposed along the principal diagonal starting from the lowest left corner. One should note that diagonal elements of the perturbation V vanish due to Eq. (6). The global structure of the matrix $H_{m,n}$ is shown in Fig. 1. The next (to the principal one) diagonals $H_{n,n\pm 1}$ correspond to transitions inside each H_0-shell while the ''arcs'' connecting the two corners represent transitions

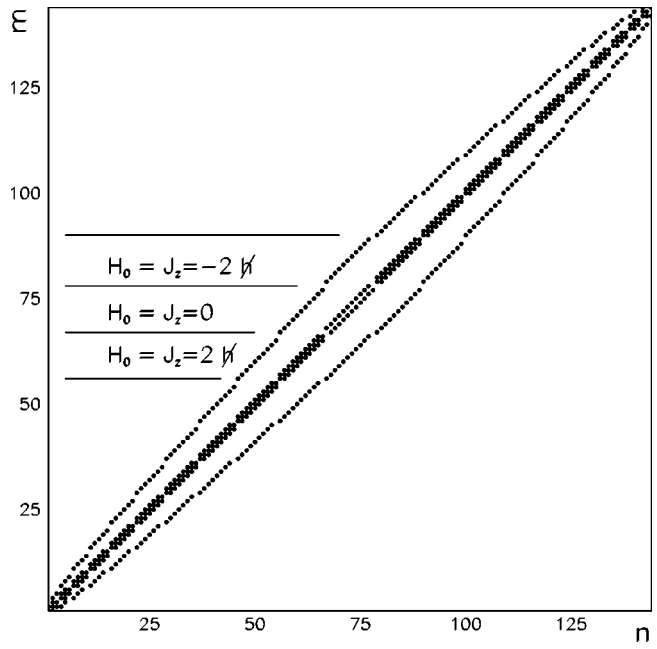

FIG. 1. Structure of the Hamiltonian matrix $H_{n,m}$ in the symmetrized basis for $l=11$ ($N=144$) and J_z even. Dots indicate off-diagonal elements different from zero. The bandwidth b is maximal at the center where $b=2l+1$. A few different H_0 shells are shown by the horizontal lines.

between neighboring shells having $\Delta H_0=\pm 2\hbar$. Such a global structure of the Hamiltonian matrix is not a peculiarity of this model but it corresponds to the so-called ''shell model'' representation widely used in atomic and nuclear physics [6,7]. It was shown in Refs. [8–10] that generic properties of eigenfunctions in this basis can be directly related to single-particle operators, in particular, with the distribution of occupation numbers for single-particle states.

The Hamiltonian matrix has a clear band structure, with the bandwidth b ranging from 1 at the corners up to $b=2l+1$ in the middle. However, this structure differs strongly from that of standard Wigner band random matrices (see, for example, [2,11] and references therein). Moreover, nonzero off-diagonal matrix elements are positive and the mean and variance of the distribution of these matrix elements depend on the classical parameter $L^2=\hbar^2 l(l+1)$ only. To be more precise, if one assumes a continuous distribution of the matrix elements, it can be shown (see Appendix A) that $\sigma^2=\langle v^2\rangle-\langle v\rangle^2\simeq(L/4)^4$.

There are of course semiclassical corrections to this estimate, but the variation of $\hbar$ in one order of magnitude (available in our numerical study) changes the ratio $\sigma^2/(L/4)^4$ by less than 1%. In the same way the mean value can be semiclassically estimated as $\langle v\rangle\simeq(\pi L/8)^2$. The agreement between these simple semiclassical formulas and our numerical data is shown in Appendix A.

The model is highly nonperturbative since the perturbation spreads the levels of the inner H_0 shell all over the allowed energy range; see Appendix B. As a result, the perturbed spectrum is broader than the unperturbed one; this is an effect of the nonzero mean value of off-diagonal matrix elements. While the unperturbed spectrum has degenerate energy levels with spacing $\hbar$ (therefore, with density of levels $\rho_0\sim 1/\hbar$ and spectral radius $R_\sigma^0=2\hbar l\sim 2L$), the perturbed one has $(l+1)^2$ nondegenerate states within a spectrum of radius $R_\sigma\sim L^2+1$, which gives the density $\rho\sim 1/\hbar^2\sim\rho_0/\hbar$.

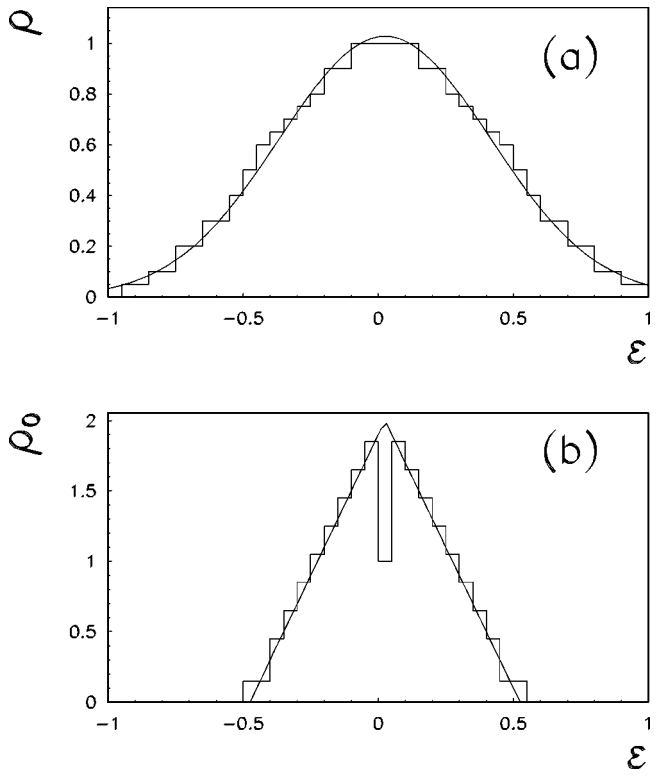

FIG. 2. Density of states for the total Hamiltonian H_0+V (a), and for the unperturbed one H_0 (b), as a function of the rescaled energy $\epsilon=E/E_{\max}$ for $l=39$ and $L=3.5$. For comparison, the fitting Gaussian (a) and the triangular curve (b) are given.

Numerical data show that the density of states changes from a triangular shape for the unperturbed Hamiltonian [one more state is added (subtracted) at each neighbor level for H_0 negative (positive)] to the Gaussian form, which is known to be generic for realistic finite systems like atoms and nuclei; see, for example, Refs. [6,7]. In Fig. 2 the perturbed and the unperturbed density are shown for a typical case, together with the corresponding fitting curves.

III. QUANTUM-CLASSICAL CORRESPONDENCE FOR EF AND LDOS

The subject of this section is the analysis of the LDOS (also known as ''strength function'' or ''Green spectra'') and of the structure of eigenfunctions, together with their classical analogs. In the quantum description, all information is contained in the matrix constructed from the eigenfunctions $\psi_n(E_m)$ of the total Hamiltonian H represented in the ordered unperturbed two-particle basis $|\mathbf{n}\rangle$. Here $\psi_n(E_m)$ is the nth component of the eigenfunction having E_m as eigenvalue. This matrix is assumed to be reordered in eigenenergies E_m.

In the classical limit the unperturbed energy E_0 is not constant when the (chaotic) trajectory of the total Hamiltonian H fills the $H=E=$const surface. Indeed it fills a range of values that are distributed according to the ergodic measure on the constant energy surface, yielding a distribution

function $W(E_0|E)$ [2]. This distribution can be easily numerically calculated taking a sample of chaotic trajectories $u(t)=(L_x(t),L_y(t),L_z(t),M_x(t),M_y(t),M_z(t))$ having the same fixed values of E and $L^2=M^2$. Following these trajectories, one can calculate $H_0(u(t))=L_z(t)+M_z(t)$ taken at equal instants of time and find the distribution of H_0 over the energy band [12] defined by sojourn times.

The quantum analog of this distribution is provided by the relation

$$W_n(E)=\langle|\psi_n(E_m)|^2\rangle_m, \tag{7}$$

where the average $\langle\cdots\rangle$ is taken over those eigenfunctions that have an eigenvalue E_m in a fixed small energy interval around a given energy E. Such an average has been done in order to smooth the fluctuations that affect individual eigenstates; we would like to note that for our dynamical model, unlike random matrix ensembles, there is no possibility of ensemble averaging. The distribution $W_n(E)$ gives the average shape of eigenstates represented in the unperturbed two-particles basis $|\mathbf{n}\rangle$.

In order to obtain the quantum distribution $W(E_0|E)$ one needs to switch to the unperturbed energy representation, $n\rightarrow E_n^0$. Technically this can be realized by introducing small energy bins ΔE and counting the correspondent probability within them,

$$W(E_0|E)=\sum_n W_n(E)\,\delta(E_0-E_n^0). \tag{8}$$

Similarly, we can define the distribution $w(E|E_0)$. In the quantum case this distribution is the LDOS defined by

$$w(E|E_0)=\sum_m \langle|\psi_n(E_m)|^2\rangle_n\,\delta(E-E_m), \tag{9}$$

where the average is now taken over a number of values of n, such that the eigenvalues E_n^0 belong to a small interval around the given unperturbed energy E_0. The presence of degeneracy in this case provides an obvious way of taking the average. The corresponding classical function can be found by noticing that the trajectory does not fill the whole surface $H_0=E_0$ but is restricted to an invariant manifold specified by the value of m. Giving equal weight to all m values corresponding to a given value of H_0 exactly matches the quantum averaging used in Eq. (9). Then the classical distribution can be evaluated analytically, since the classical unperturbed Hamiltonian H_0 is integrable. Indeed, the unperturbed solution $u_0(t)$ for $L^2=M^2$ and $H_0=0$ is given explicitly by

$$L_x^0(t)=\sqrt{L^2-m^2}\cos 2(t-\phi),$$

$$L_y^0(t)=\sqrt{L^2-m^2}\sin 2(t-\phi),\quad L_z^0(t)=m,$$

$$M_x^0(t)=\sqrt{L^2-m^2}\cos 2(t-\xi),$$

$$M_y^0(t)=\sqrt{L^2-m^2}\sin 2(t-\xi),\quad M_z^0(t)=-m, \tag{10}$$

where $0<\phi<2\pi$, $0<\xi<2\pi$, and $|m|\leq L$ depend on the initial conditions. Therefore,

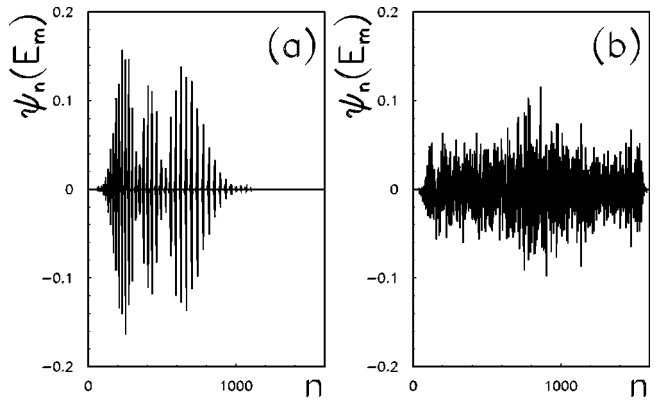

FIG. 3. Typical eigenfunctions for the case $L=3.5$, $l=39$. (a) The second excited state $\psi_n(E_2)$ (corresponding to a classically integrable region). (b) Eigenfunction for the energy E_m close to zero (middle of the spectrum, corresponding to the chaotic region).

$$H(u_0(t))=(L^2-m^2)\cos 2(t-\phi)\cos 2(t-\xi).$$

This means that the classical distribution of H is given by $P_L(y)$ where $y=L^2(1-x_1^2)\cos\pi x_2\cos\pi x_3$ is a function of the random variables $-1<x_i<1$, $i=1,2,3$.

IV. STRUCTURE OF EIGENFUNCTIONS

The quantum model has been already studied in Ref. [5], but previous studies have not addressed the structure of eigenfunctions in the two-body particle basis. This representation is quite natural and corresponds to a well-known procedure in the physics of interacting particles.

In our dynamical model the structure of eigenfunctions strongly depends on their energy because in the classical limit for low and high energies ($|\epsilon|=|E|/E_{\max}\sim 1$) the motion is regular while in the center of the energy band ($|\epsilon|\sim 0$) is chaotic. One can, therefore, expect that in the classical limit ($\hbar\sim L/l\ll 1$) the eigenstates corresponding to regular or chaotic regions are very different. This is, indeed, clearly seen in Fig. 3 where two eigenstates are plotted in the unperturbed two-particle basis for the second (from the bottom of the spectrum) eigenstate ($\epsilon\sim -1$) and for the eigenstate chosen in the center of the energy band ($\epsilon\sim 0$). Comparing these two (typical) eigenstates, one can see that there are strong correlations between components of the ''regular'' one [Fig. 3(a)] while the ''chaotic'' eigenstate can be treated as random along the whole basis $|\mathbf{n}\rangle$. We also would like to note that the regular eigenstate has many ''principal components'' and that it looks more or less extended. This again indicates that the perturbation is quite strong and effectively couples many unperturbed states.

A much more accurate analysis of eigenfunctions is obtained by studying their localization lengths. Since the basis is finite and eigenstates can be extended along it, here we use different measures of localization lengths, based on their entropy $\mathcal{H}$ and participation ratio $\mathcal{P}$ see, e.g., Refs. [13,14],

$$l_H(E)=2.08\exp\{-\mathcal{H}\},\quad l_{\rm ipr}(E)=3/\mathcal{P}, \tag{11}$$

where

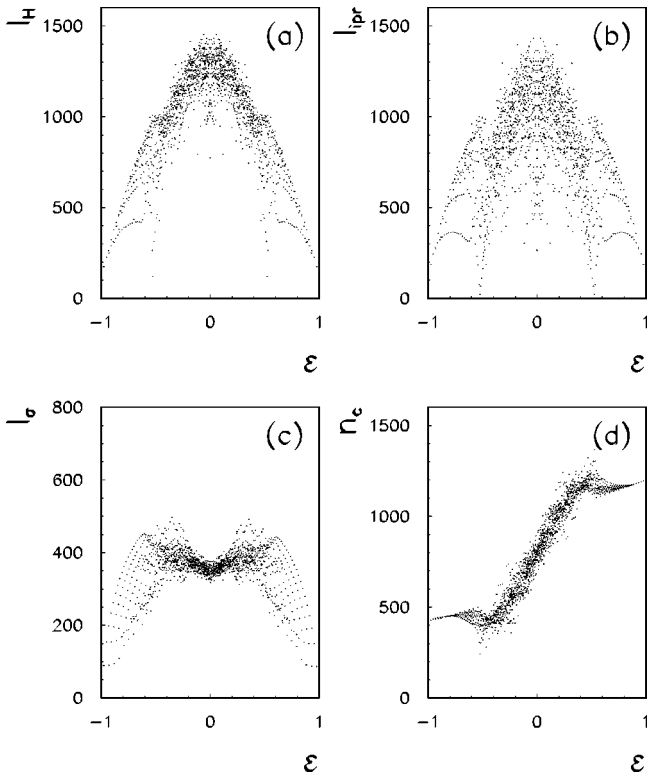

FIG. 4. Measures of localization lengths for eigenfunctions vs the rescaled energy for the case $L=3.5, l=39$. (a) Entropy localization length l_H (b) localization length $l_{\rm ipr}$ defined as the inverse participation ratio, (c) square root of the variance, l_σ, (d) centroid n_c.

$$\mathcal{H}=\sum_{n=1}^{N} |\psi_n(E)|^2 \ln|\psi_n(E)|^2$$

and

$$\mathcal{P}=\sum_{n=1}^{N} |\psi_n(E)|^4.$$

The normalizing coefficients 2.08 and 3 were chosen in order that $l_H=l_{\rm ipr}=N$ in the limit case when all components $\psi_n(E_m)$ are independent Gaussian random variables. Here $N=(l+1)^2$ is the size of the two-particle basis.

Further information can be extracted from the centroids n_c of eigenstates and from their ''widths'':

$$n_c(E)=\sum_n n|\psi_n(E)|^2,$$

$$l_\sigma(E)=\left\{\sum_n |\psi_n(E)|^2[n-n_c(E)]^2\right\}^{1/2}. \qquad (12)$$

In Fig. 4 we present numerical results for the above quantities as functions of the rescaled energy ϵ.

First, we note that the entropy and inverse participation ratio localization lengths, l_H and $l_{\rm ipr}$, are approximately equal and show the same behavior, namely, the delocalization along the whole basis in the middle of the spectrum, and the localization at the spectrum edges [see Figs. 4(a)–(b)]. We also note that due to the underlying symmetry of the model the above quantities $l_{\rm ipr}, l_{\mathcal{H}}$ are symmetric around $\epsilon=0$.

Even in the center of the spectrum, where eigenstates are on average maximally extended, there are large fluctuations in the value of localization lengths. This indicates that in the classically chaotic region there are some eigenstates that cannot be treated as completely random and delocalized over the energy shell. A careful study shows that such eigenstates are characterized by an extended background with some pronounced peaks (the so-called ''sparse eigenstates''). Such eigenstates may result in the absence of equilibrium and in the lack of standard statistical description, see details in Ref. [9].

One can also see a clear regular structure in the dependence of l_H and $l_{\rm ipr}$ on the energy at the edges of the spectrum, which reflects the regular character of eigenstates.

The other two quantities, n_c, l_σ, give information about the ''position'' and ''width'' of eigenfunctions in the two-particle basis, see Figs. 4(c) and (d). In contrast to l_H and $l_{\rm ipr}$ the ''width'' l_σ reveals a quite unexpected minimum at the center of the spectrum. Additional numerical analysis shows that this is a result of different ''sparsity'' of chaotic states depending on the energy. Namely, chaotic eigenstates are more compact at the center of the energy band than far from it. In fact, the ratio $l_\sigma/l_{H,\rm ipr}$ can be used to extract any information about the sparsity of eigenstates (see Ref. [15]). Indeed, two eigenstates with the same value of $l_{H,\rm ipr}$ can have very different values of l_σ depending on whether principal components [those with relatively large values of $\psi_n(E_m)$] are clustering around some center (small l_σ) or randomly scattered over the whole unperturbed basis (large l_σ).

Additional information can be obtained from the dependence of the centroids of eigenstates on the energy, see Fig. 4(d). Apart from fluctuations and excluding the regular part, this dependence is linear, which means that, on average, centers of eigenstates are located at the center of the energy shell covered by the classical distribution $w(E|E_0)$. This generic feature of chaotic eigenstates has been studied in greater details in WBRM models [2]. In particular, it was shown that those eigenstates, which are completely extended in the whole energy shell, are characterized by maximal statistical properties of quantum chaos. For example, in that case the statistics of the energy spectrum follows the predictions of random matrix theory, such as the Wigner-Dyson form of the distribution of spacings between neighboring energy levels. On the other hand, localization of eigenstates within the energy shell leads to the so-called intermediate statistics [13] (which is intermediate between the Wigner-Dyson and the Poisson statistics).

Such a localization is reflected in the fluctuations of n_c around the center of the shell (linear dependence on ϵ). Indeed, if eigenstates are localized, their centers n_c are typically scattered within the energy shell leading to strong fluctuations of n_c; instead, this cannot happen if they fill the whole energy shell. It is important to stress that localization in the energy shell is different from that in the unperturbed basis, as found from Eqs. (11).

The result presented in Fig. 4(d) shows that localization in the energy shell, if any, is quite weak. A more direct analysis of the degree of localization in the energy shell is provided

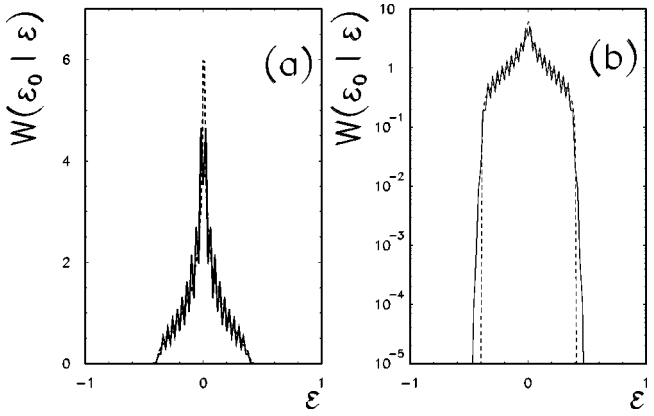

FIG. 5. (a) Shape of eigenfunctions in the energy representation (full line) and classical distribution $W(\epsilon_0|\epsilon)$ (dashed) for the case $L=3,5l=39$, obtained by averaging over the central $l+1$ eigenfunctions with $\epsilon_0=0$; (b) the same plot in semilog scale.

by direct comparison of the average shape of eigenstates in energy representation to its classical analog. The results are presented in Fig. 5 where quantum and classical $W(E_0|E)$ [see Eq. (8)] are plotted versus the rescaled energy $\epsilon = E/E_{\max}$.

One can see that the only important difference is a sort of a weak quantum tunneling in the classically forbidden region (the tails of the classical distribution are sharper than the quantum ones). Anyway, the good correspondence between quantum and classical distributions shows that for the chosen parameters the model is in a deep semiclassical region and, globally, the eigenstates should be treated as ergodic ones (in the energy shell, not in the whole unperturbed basis!). This means that the observed scattering of the centroids of eigenstates [see Fig. 4(d)] is, in fact, quite weak and does not lead to noticeable localization in the energy space.

Interestingly, the size of these ergodic eigenfunctions is smaller than the total-energy band. The distribution W_0 is in fact restricted between the minimum and the maximum values that the function $H_0=L_z+M_z$ can assume under the constraints $E=L_z+M_z+L_xM_x$, $L_x^2+L_y^2+L_z^2=M_x^2+M_y^2+M_z^2=L^2$. It can be easily proved, using the Lagrange multipliers methods that for $E=0$, $|E_0|<2(\sqrt{L^2+1}-1)$, which in Fig. 5 corresponds to $|\mathrm{Supp}W(\epsilon_0|\epsilon)|<\tilde{\epsilon}\simeq 0.398$.

V. LDOS STRUCTURE

Of special interest is the structure of LDOS, which is widely discussed in many applications in atomic, nuclear, and solid-states physics. The importance of this quantity relates to its physical meaning: it shows how an unperturbed state $|\mathbf{n}\rangle$ ''decays'' into other states due to interaction. In particular, the inverse width of the LDOS is associated with the mean ''lifetime'' of a chosen basis state.

As was indicated above, the LDOS structure can be extracted from the matrix $\psi_n(E_m)$ by fixing an unperturbed state $|\mathbf{n}\rangle$ and searching the dependence on m. Therefore, we can adopt the same procedure as we did above when analyzing the structure of eigenstates. In comparison with Fig. 3 we show two such ''matrix lines'' corresponding to basis states (BS's), with close n values, taken from the center of matrix (see Fig. 6). In fact, the BS lines in this matrix correspond to

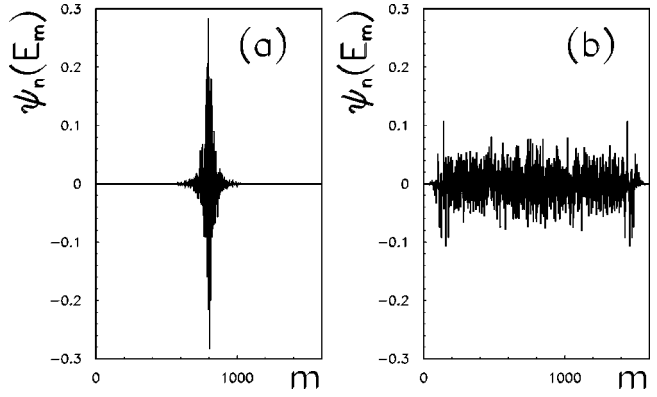

FIG. 6. (a) The BS for an n value corresponding to a shell edge indicated as a dashed line in Fig. 8. (b) The BS in the middle of $H_0=0$ shell.

the expansion of unperturbed (basis) states in the exact eigenstates. While the structure represented in Fig. 6(b) is typical, the form of the BS in Fig. 6(a) is only observed around some specific value of n.

To better understand the meaning of these peculiar n values we have computed the localization length [compare with Eq. (11)]

$$l_{\mathrm{ipr}}(n)=3/\sum_m |\psi_n(E_m)|^4 \tag{13}$$

in some range of n. The data presented in Fig. 7 reveal a global periodic structure of BS's, from which one understands that the peculiarity of BS's reflected in Fig. 6 results from the degeneracy (inside each shell) of the unperturbed spectrum. It is then convenient to consider in the following analysis, as a reference, the central shell $H_0=0$ only (set of $l+1$ BS).

Now we discuss the structure of the BS in energy space which is, in fact, the LDOS [Eq. (9)]. According to results [11] obtained for WBRM, the shape of the LDOS typically changes from the Breit-Wigner (BW) law to the semicircle when an effective perturbation is increased. In particular, the BW is expected when

$$1/\sqrt{2\pi} \ll \rho_0 V \ll \sqrt{b/2\pi}, \tag{14}$$

where ρ_0 is the density of the unperturbed spectrum and b is the effective bandwidth of the Hamiltonian matrix. The first inequality is related to the nonperturbative character of the coupling (which is always verified in this model) while the last, rewritten as

$$2\pi\rho_0 V^2=\Gamma_F \ll b/\rho_0,$$

simply means that the spreading width Γ_F of such distribution has to be much smaller than the energy bandwidth b/ρ_0. If we formally apply the above conditions to our case, we get (in units of $\epsilon=E/E_{\max}$) the following relations: $b/\rho_0\simeq 1/L$ and $2\pi\rho_0V^2\simeq(\pi/2)(L/4)^3l$. With our data the second condition in Eq. (14) is strongly violated. In fact, the random matrix argument leading to the above results rests on the assumption that the band in the Hamiltonian matrix be

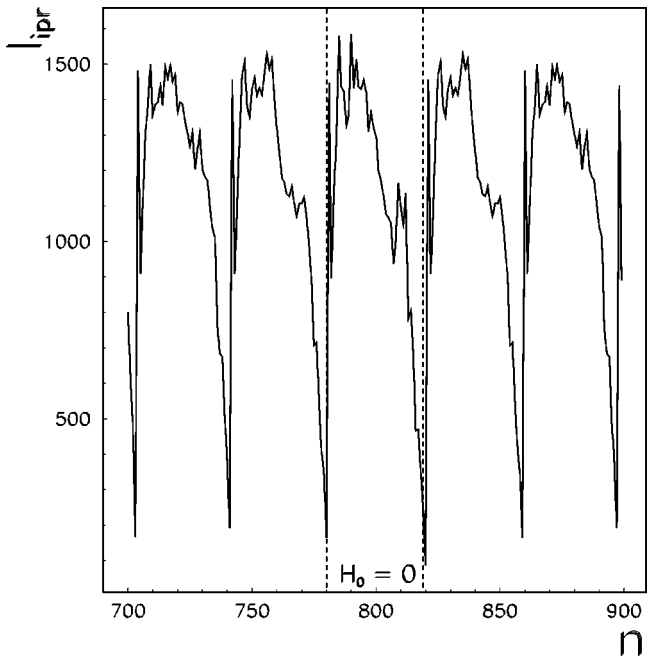

FIG. 7. Dependence of the inverse participation ratio of the nth BS of the H matrix as a function of n. Here is $L=3.5, l=39$. The $H_0=0$ shell is inside the two vertical dashed lines.

''full''; in our case, instead, we have a large sparsity (many vanishing matrix elements inside the band).

In Fig. 8 we show the structure of the LDOS for the BS corresponding to the center of the unperturbed spectrum, in comparison with the Breit-Wigner fit which is performed within the interval $(-b/2\rho_0, b/2\rho_0)$.

One should stress that outside of the energy interval corresponding to the band size, the tails of the LDOS are known to be highly nongeneric [6,11,16,7] depending on specific properties of the model. As one can see, inside this energy interval the shape of the LDOS can be roughly associated with the BW form. On the other hand, outside, the tails decay very slowly compared to those given by the BW. Such a form of the tails is also different from the case of the WBRM [6], where outside the band energy range the tails decay extremely fast (even faster than exponential). In general, the above results seem to indicate that the effective perturbation corresponds just to the condition when the BW approximation starts to fail.

Let us now compare the quantum and classical LDOS. In Fig. 8 we give an example of such distributions in the whole energy shell. They coincide with a high accuracy, apart from the regions very close to the energy shell edges (where quantum tunneling is significant).

This again means that the system is in a deep semiclassical regime. We remark that, in this model, going to the quantum regime in the chaotic energy region calls for very small matrices, for which fluctuations are extremely strong.

An important question is the relevance of the shape of eigenstates to that of the LDOS. As was shown in the model of WBRM [17] in some range of parameters (for not very strong perturbation) the two shapes are very close to each other, which is a manifestation of the ergodic structure of eigenstates in the energy shell. On the other hand, with an increase of perturbation the LDOS was found to tend to the

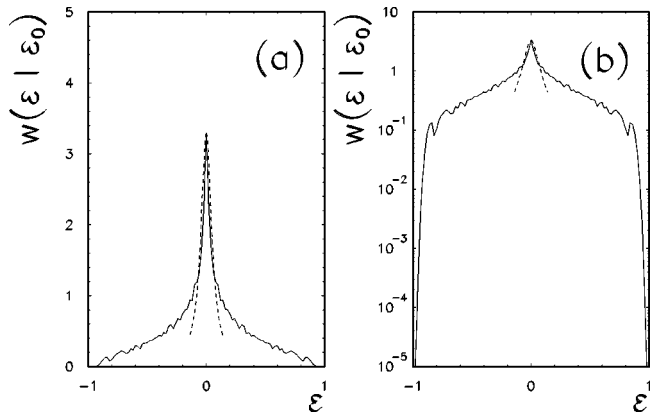

FIG. 8. (a) Quantum LDOS distribution $w(\epsilon|\epsilon_0) = w(E/E_{\max}|E_0/E_{\max})$ (full line) and best-fitted Breit-Wigner distribution in the range specified above (dashed line) for the case $L=3.5, l=39$, obtained averaging over $l+1$ values of BS for the $H_0=0$ shell; (b) the same plot in semilog scale.

semicircle, for which strong localization turns out to be possible [2]. This localization manifests itself in different average shapes of the EF and LDOS. Namely, the width of the EF in the energy representation is less than the width of the LDOS; the latter defines, in fact, the width of the whole energy shell.

Direct comparison of Fig. 5 and Fig. 9 in our dynamical model shows a remarkable different energy range for the LDOS and EF distribution. As was discussed above, the energy width of eigenfunctions in the semiclassical region (in the energy representation), is much smaller than the width of the spectrum because it is subject to an additional constraint. We can take into account this restriction and rescale the distribution $W(\epsilon_0|\epsilon)$ in order to have the same energy range as for $w(\epsilon|\epsilon_0)$: $W_r(\epsilon_0|\epsilon) = \tilde{\epsilon} W(\epsilon_0/\tilde{\epsilon}|\epsilon/\tilde{\epsilon})$ where $\tilde{\epsilon} = 2(\sqrt{L^2+1}-1)$. The rescaled distribution W_r is presented in Fig. 10 together with the distribution $w(\epsilon|\epsilon_0)$. After such a rescaling both distributions coincide quite well, which again indicates the absence of the localization.

VI. RANDOM TWO-BODY INTERACTION

In this section we modify our model of two interacting particles by assuming a completely random interaction that

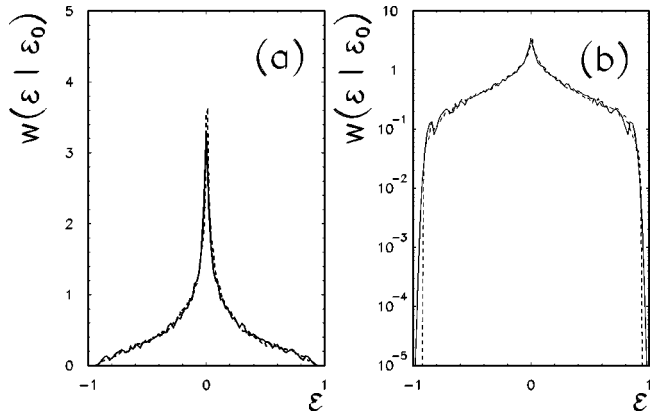

FIG. 9. (a) The LDOS distribution $w(\epsilon|\epsilon_0)$: quantum (full line) and classical (dashed line) for the case $L=3.5, l=39$, obtained by averaging over $l+1$ values of BS for $H_0=0$ shell; (b) the same plot in semilog scale.

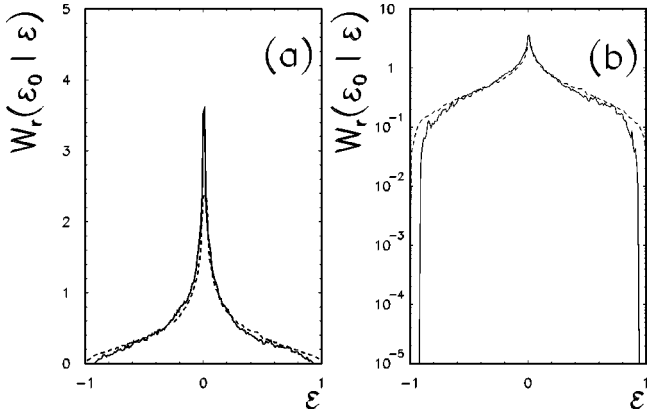

FIG. 10. (a) Classical LDOS distribution $w(\epsilon,\epsilon_0)$ (full line) and the rescaled classical distribution $W_r(\epsilon_0|\epsilon)$ for the case $L=3.5, l=39$; (b) the same plot in semilog scale.

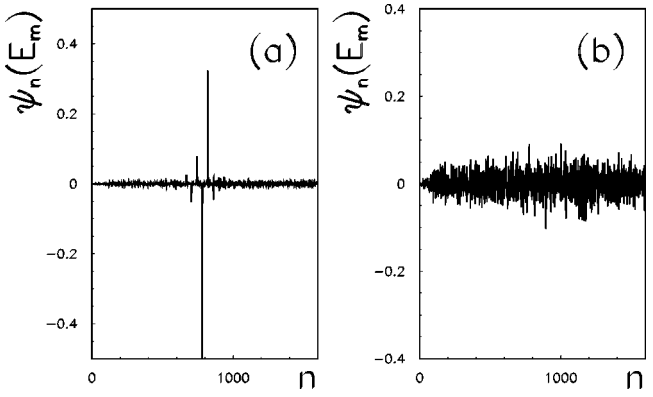

FIG. 11. Typical eigenstates for the case $L=3.5$ and $l=39$ and Gaussian random nonzero off-diagonal elements. (a) and (b) have close eigenvalues in the middle of the spectrum, respectively, $\epsilon = E/E_{\max} = 1.48\times10^{-3}$ and $\epsilon = E/E_{\max} = 2.295\times10^{-2}$ but very different inverse participation ratios ($l_{\rm ipr}/N = 0.0027$ for the first and $l_{\rm ipr}/N = 0.87$ for the last, where N is the matrix size).

preserves some global properties of the original dynamical model (1). Namely, the unperturbed part H_0 is taken to be exactly the same as in the dynamical model. However, we replace nonzero matrix elements of the dynamical model with random and independent variables. Moreover, we choose a Gaussian distribution of these random matrix elements with the same mean and variance as for the dynamical elements. In such a way we can reveal the influence of dynamical correlations that are due to the specific form of the interaction V. Below we follow the same procedure described in previous sections when studying eigenstates and LDOS.

Numerical data for the ''randomized'' model show that global spectral properties are the same as in the dynamical model. Namely, the perturbed spectrum is enlarged with respect to the unperturbed one and the density of states keeps the same Gaussian shape with the same mean and variance.

On the other hand, the analysis of eigenfunctions reveals clear differences. Typical shapes of eigenstates and BS are shown in Fig. 11. In comparison with the corresponding Fig. 3(b), one notes that extended states look chaotic, similar to those found in the dynamical model. However, differently from the dynamical model, a few strongly localized states now appear even in the center of the energy band. A typical example of such an eigenstate is given in Fig. 11(a).

To analyze the global characteristics of all eigenstates we have calculated different localization lengths l_H and $l_{\rm ipr}$ as well as the width l_σ and the centroids n_c according to Eqs. (11) and (12). The data reported in Fig. 12 should be compared with those in Fig. 4 for the dynamical model. As expected, for the random model there are no correlations in the energy dependence for large or small energy ($|\epsilon| \simeq 1$), compared with Fig. 4. However, close to the edges of the energy spectrum, the eigenstates cannot be treated as chaotic since the number of ''principal components'' in such eigenstates is quite small (this is revealed by small values of localizations lengths $l_H, l_{\rm ipr}, l_\sigma$). This is a result of the perturbative localization that typically occurs for states close to the ground state. In what follows, we exclude such states from our consideration.

For chaotic eigenstates, the various measures of localization lengths give average values typically less than in the dynamical case. This holds especially in the middle of the spectrum $E \simeq 0$ where we can now find a relatively large number of sharply localized eigenstates (with $l_{\rm ipr}/N \ll 0.1$ where N is the matrix size), see Fig. 11(a). In the same Fig. 12(d) one can also observe a much stronger scatter of the centroids of eigenstates transverse to the diagonal [compare with Fig. 4(d) of the dynamical model]. The same features have been found for basis states. These data indicate that fluctuations in the structure of eigenstates are much stronger than in the dynamical model.

Despite these fluctuations, the global structure of the EF seems to remain the same. This is marked once more by the distribution of eigenfunctions in the energy space (the analog of Fig. 5 is now shown in Fig. 13) which has the same shape as in the dynamical model. However, the LDOS distribution for the random model shows striking difference, see Fig. 14. Indeed, it can be described, apart from the central peak, by the semicircle law [3,11,2]. Due to numerical problems, we are not able to resolve the finite-size corrections close to the energy band, studied in Ref. [16].

This surprising result is quite significant in the light of application of random matrix models. Indeed, in Refs. [18,19,2] it was found that localization in the energy shell for the WBRM may occur only when the LDOS is characterized by the semicircle law. Therefore, the important question is whether the semicircle law is a quantum feature or it can also occur in classical dynamical conservative systems. What we have found here is that the semicircle law has nothing to do with the semiclassical limit in our model. It seems to be dictated by quantum randomness rather than by the pseudo-randomness resulting from the classical chaos.

By comparing the shapes of the LDOS and EF for the random model, one can see that they are clearly different, in contrast to the dynamical model. As mentioned above, in Ref. [2] such a difference was directly connected to the localization of eigenstates in the energy space. As a result of this localization, the spectrum statistics differs from that predicted by the RMT. In particular, for Wigner band random matrices, the level spacing distribution was found [2] to deviate from the Wigner-Dyson dependence.

To check these predictions, we have calculated the level spacing distribution for both dynamical and random models

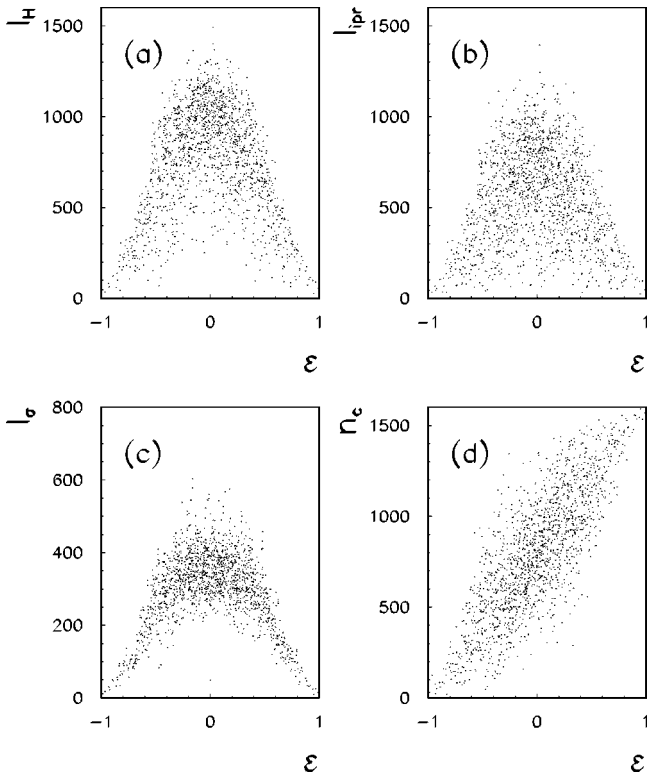

FIG. 12. Measures of localization lengths for eigenfunctions for the Gaussian random case $L=3.5, l=39$; compare with Fig. 5.

for the part of the spectrum corresponding to chaotic eigenstates. As we expected, for the dynamical model we have observed a very good correspondence to the Wigner-Dyson dependence. Surprisingly, we have found that the random model gives the same result. This means that the level spacing distribution is quite insensitive to the small number of localized eigenstates. On the other hand, this result indicates that, in the case of realistic matrices, the degree of level repulsion is not so clearly affected by the difference in the shapes of the LDOS and EF, as it was in the case of WBRM.

VII. SUMMARY

In this paper we have studied a dynamical model with two interacting particles (rotators). The classical version of this model manifests both regular and chaotic motion, depending on the total energy: both at small and at large energies the motion is regular, while, at intermediate energies, chaotic properties are very strong. The quantum analog of this model can be assumed to describe two interacting spins. Our choice was restricted to the subset of symmetric states, which corresponds to particles with integer spins.

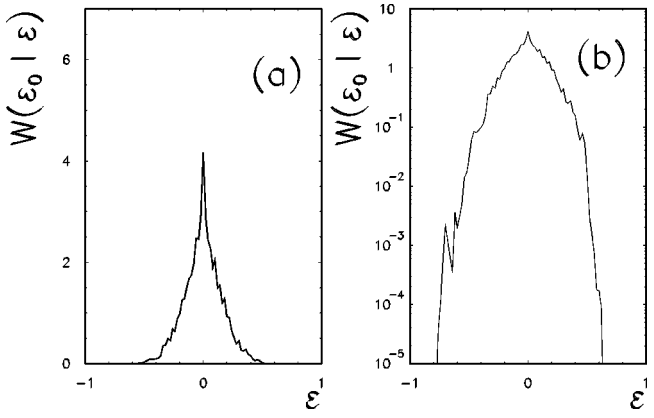

FIG. 13. (a) The EF distribution for the Gaussian random case with $L=3.5, l=39$, obtained by averaging over $l+1$ central eigenfunctions; (b) the same as (a) in semilog scale.

This model has already been under investigation, both in the classical and in the quantum description (see, for example, Ref. [4]). However, here we have used an approach that seems much more instructive: in the quantum case, we have represented the Hamiltonian matrix in the basis defined by the two-body eigenstates of the noninteracting system, reordered according to increasing total energy. Such a representation corresponds to a well-known procedure in atomic and nuclear physics (''shell-basis representation''), and seems to be very useful in view of recent developments [8,9].

In this representation the Hamiltonian matrix turns out to be banded, with many zero elements inside the band. If pseudorandomness of nonzero off-diagonal elements is assumed (in the region of classical chaos), then one can refer to some modern developments of random matrix theory: in particular, to the so-called Wigner band random matrix ensemble, which is conjectured to be well suited to the description of conservative systems with complex behavior (see Ref. [2] and references therein). However, the assumption of pseudorandomness of matrix elements is far from obvious: checking it was in fact one of the major motivations of our work.

Random matrices in the WBRM ensemble are characterized by a sharp band inside which matrix elements are random, independent, and identically distributed, plus an additional principal diagonal with increasing entries, corresponding to the unperturbed spectrum of the two-body Hamiltonian.

Compared to WBRM, our model has two peculiarities. In the first place there is no free parameter of interaction between the particles, the only parameter that determines the relative strength of the interaction being the total energy of the system. Second, our model has an highly degenerate unperturbed spectrum. Still, the main features of the model are expected to be quite generic, because these peculiarities are quite typical in such physical applications as complex atoms and nuclei.

In this paper we have analyzed two main issues, motivated by recent results [2,8,9]. First, we have studied the structure of the eigenfunctions and of the LDOS and have compared them to what is known for completely random models, and for WBRM in particular. Second, we have looked for effects of dynamical localization; though we have found no significant evidence for such effects, our analysis has brought into light a close connection (surmised in Ref. [2]) between the LDOS, eigenfunctions, and certain classical distributions, which can be easily found by solving the classical equations of motion.

As expected, in the region of classical regular motion, eigenstates have a regular structure themselves; still, classical integrability does not result in strong localization, because these eigenstates are typically quite extended over the basis of two-particle unperturbed states. In contrast, in the region of classical chaos, the structure of eigenstates looks

very chaotic itself. Nevertheless, the size of such chaotic eigenstates can be smaller than the size of the basis, though the eigenstates may be treated as random (ergodic) ones on the scale of their localization.

The dependence of the structure of eigenstates on energy reflects their regular or chaotic nature, as it is chaotic itself in the latter case; e.g., fluctuations of the number of principal components are stronger where classical chaos is stronger, which is the reason why a non-negligible fraction of eigenstates have a size significantly smaller than the basis size.

Generally speaking, the global properties of chaotic eigenstates are quite similar to those found for WBRM, with one remarkable exception. In fact, for the WBRM ensemble, the expansion of exact eigenstates over the unpertubed ones has a structure quite similar to the one observed on expanding unperturbed eigenstates on the basis of exact eigenstates. Instead, this symmetry is broken in our model, apparently due to the degeneracy of the unperturbed spectrum: a feature that is missing in WBRM.

Expansion of unperturbed eigenstates on exact ones directly leads to the LDOS. In standard random matrix models the latter is known to be of the BW type, with the half-width given by the Fermi golden rule. Instead, in our dynamical model the LDOS is BW like only around the central peak; its tails have a much slower decay than predicted by the BW law.

Dynamical localization effects are an extremely important issue when investigating the quantum mechanics of chaotic systems. Our approach to this problem was based on Ref. [2], where it was argued that, for the case of conservative systems, such effects are manifested by localization of eigenstates within the so-called energy shell, which is the range of energies ergodically explored by classical motion. From this viewpoint, in order to detect localization (if any), one has to find the form of the classical energy shell, and then to compare it with the form of chaotic quantum eigenstates.

Following this approach, we have defined and numerically computed classical distributions that strikingly correspond to the LDOS and to the average shape of eigenfunctions. Besides opening a new direction in the study of the global properties of the quantum LDOS and EF's, this fact may be important for the quantum statistical mechanics of isolated, chaotic systems of interacting particles, because the knowledge of the average shape of eigenstates gives analytical access to the distribution of occupation numbers of single-particle states [8,9]. However, insofar as localization effects are concerned, the close agreement we have observed between quantum and classical distributions indicates that no such effect is present in our model, which is, in fact, in a deep quasiclassical region. Additional indications of absence of significant localization effects is provided by the analysis of the level-spacing distribution, which closely follows, in the strongly chaotic case, the predictions of random matrix theory.

Finally, we have studied a random matrix analog of our dynamical model, which was constructed by leaving the unperturbed part of the Hamiltonian matrix unaltered and by replacing all nonzero off-diagonal elements by Gaussian random variables with the same mean and variance as in the dynamical model. In this way we were able to check to what extent quantum chaotic dynamics can be simulated by random interactions; in other words, we have checked the pseudorandomness assumption. We have found that the random matrix model and the dynamical one are very similar in what concerns the global average properties of eigenstates. Nevertheless we have found that fluctuations of individual eigenstates are significantly stronger in the random model: in particular, there are many more eigenstates that are significantly more localized in comparison to the average size of chaotic eigenstates. In spite of this enhancement of the number of localized states, the level spacing distribution of the random model is still short of showing significant deviations from random matrix theory.

The most striking difference between the dynamical and the random model has been detected in the form of the LDOS. The LDOS of the random model drastically differs from that of the dynamical model, as it is quite close to the semicircle law, with an additional peak at the center. While the origin of this peak is related to a specific feature of our model, the occurrence of the semicircle is somewhat surprising, because the general statistical properties of the random model are similar to those of the dynamical one. For WBRM, the semicircle law appears when the perturbation (that is, the variance of the off-diagonal elements) is strong; moreover, localization in the energy shell was found to appear only in the presence of the semicircle law. In contrast to the dynamical model, neither WBRM nor the random model have a classical analog (although the latter is much closer to a realistic systems than WBRM); therefore one can ask the question of whether the semicircle law for the LDOS can appear at all in quantum systems with a chaotic classical limit. Our analysis shows that great care has to be taken in extending predictions of random matrix theory to systems of the latter class, at least if the systems themselves are in a quasiclassical regime. In that case the pseudorandomness assumption obliterates dynamical correlations to which the LDOS, and similar quantities, are quite sensitive.

ACKNOWLEDGMENTS

F.M.I. thanks, with pleasure, the colleagues of the University of Milan at Como for their hospitality during his visit when this work was done; he acknowledges the support from the Cariplo Foundation for Research grant, and partial support from INTAS Grant No. 94-2058.

APPENDIX A

In this appendix we show that assuming a continuous distribution of off-diagonal nonzero elements, the average and variance can be estimated semiclassically and good agreement with numerical data is found. Let us start with Eq. (6), from which we have

$$\langle v\rangle = \frac{\hbar^2}{M^2}\sum_{i=1}^{M}\sum_{j=1}^{M}\left[(i+l)(i-l+1)(j+l)(j-l+1)\right]^{1/2}$$

$$\simeq \frac{\hbar^2}{16l^2}\int_{-l}^{l} dx\,\sqrt{(x^2-l^2)}\int_{-l}^{l} dy\,\sqrt{(y^2-l^2)}, \qquad \text{(A1)}$$

where, as usual $L^2=\hbar^2 l(l+1)$. Integrals can be easily evaluated and one has

$$\langle v\rangle \simeq \left(\frac{\hbar l\pi}{8}\right)^2 \simeq \left(\frac{\pi L}{8}\right)^2. \tag{A2}$$

In the same way,

$$\langle v^2\rangle = \left(\frac{\hbar^2}{4M}\right)^2 \sum_{i=1}^{M}(i^2-l^2)\sum_{j=1}^{M}(j^2-l^2)$$

$$\simeq \left(\frac{\hbar}{2}\right)^4\left[\frac{1}{2l}\int_{-l}^{l}dx(l^2-x^2)\right]^2$$

$$= \left(\frac{\hbar^2 l^2}{6}\right)^2 \simeq \left(\frac{L^2}{6}\right)^2, \tag{A3}$$

in such a way that

$$\sigma^2 = \langle v^2\rangle - \langle v\rangle^2 \simeq \left(\frac{L}{4}\right)^4. \tag{A4}$$

The agreement between Eqs. (A2) and (A4) and numerical data is shown in Fig. 15.

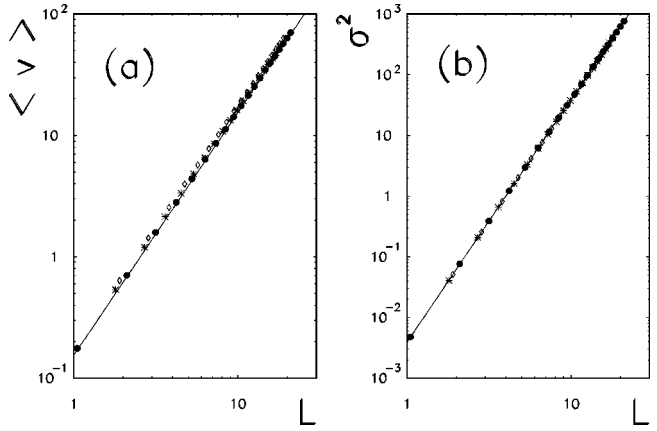

FIG. 15. (a) Off diagonal nonzero matrix elements average as a function of classical L and $l=9$ (circles), $l=19$ (squares), $l=39$ (crosses); the line is the semiclassical expression $(\pi L/8)^2$. (b) Off-diagonal nonzero matrix elements variance as a function of classical L and $l=9$ (circles), $l=19$ (squares), $l=39$ (crosses); the line is the semiclassical expression $(L/4)^2$.

APPENDIX B

It is instructive to estimate the splitting of the energy levels within one H_0 shell due to the perturbation, using degenerate perturbation theory. Let us consider, for instance, a shell with $H_0=2\hbar j>0$ that has degeneracy $p=l+1-j$. Perturbed energy levels can be calculated by diagonalizing the matrix:

$$h_{s,s'} = \langle s, 2j-s|V|s', 2j-s'\rangle. \tag{B1}$$

This is a symmetric tridiagonal matrix with zero elements along the principal diagonal, whose elements for any $s\geqslant 2$ are given by

$$h_{s,s+1} = \frac{\hbar^2}{4}\sqrt{[(l-s+1)^2-j^2][(l+s)^2-j^2]}. \tag{B2}$$

The distance between two neighboring perturbed levels can be estimated as the difference between two neighboring matrix elements (due to the symmetry of the matrix),

$$h_{s+1,s+2} - h_{s,s+1} \sim \frac{\hbar^2}{2}l, \tag{B3}$$

where the approximation is taken for $j=s=0$. This means that the total splitting is of the order

$$\Delta E \sim 2pl\hbar^2/2 \sim \hbar^2 l^2 \sim L^2. \tag{B4}$$

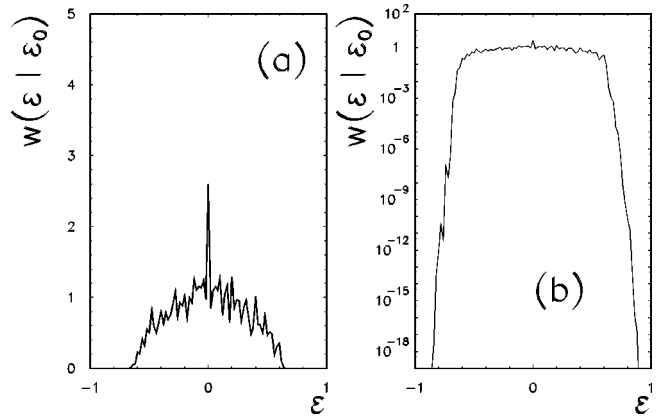

FIG. 14. (a) The LDOS distribution for the Gaussian random case with $L=3.5, l=39$, obtained by averaging over $l+1$ central lines; (b) the same as (a) in semilog scale.

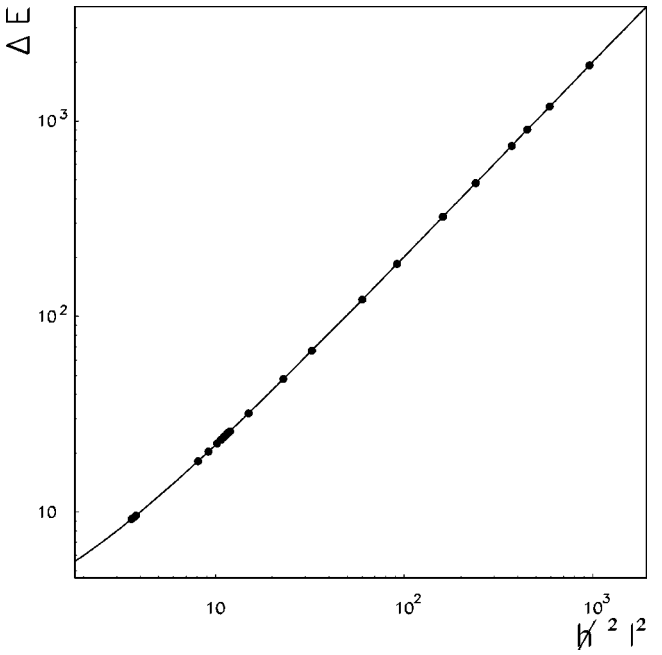

FIG. 16. Energy spectrum splitting ΔE due to the perturbation V, as a function of $\hbar^2 l^2$ for $0.01<\hbar<2$, $l<40$, and $L>1$ (points). Full line is the classical energy shell $\Delta E = 2(L^2+1)$.

Though this approximation is obtained for $j=0$, corresponding to the biggest H_0 shell, similar behavior is expected for other shells. The expression (B4) has been checked numerically; see Fig. 16, where we plot $\Delta E=E_u-E_l$ as a function of $\hbar^2 l^2$ for different l and $\hbar$ (here E_u and E_l are the energy of the upper and lower split level within one H_0 shell) For comparison, in Fig. 16, the relation $\Delta E=2(1+\hbar^2 l^2)$ is also shown, which, in the classical limit $\hbar\to 0$, $l\to\infty$, and for $L>1$ yields the expression for the classical energy shell, $\Delta E=2E_{\max}=2(1+L^2)$.

[1] B. V. Chirikov, F. M. Izrailev, and D. L. Shepelyansky, Sov. Sci. Rev. **2C**, 209 (1981).

[2] G. Casati, B. V. Chirikov, I. Guarneri, and F. M. Izrailev, Phys. Lett. A **223**, 430 (1996).

[3] E. Wigner, Ann. Math. **62**, 548 (1955); **65**, 203 (1957).

[4] M. Feingold and A. Peres, Physica D **9**, 433 (1983).

[5] M. Feingold, N. Moiseyev, and A. Peres, Phys. Rev. A **30**, 509 (1984); A. Peres, Phys. Rev. Lett. **53**, 1711 (1984).

[6] V. V. Flambaum, A. A. Gribakina, G. F. Gribakin, and M. G. Kozlov, Phys. Rev. A **50**, 267 (1994).

[7] N. Frazier, B. A. Brown, and V. Zelevinsky, Phys. Rep. **276**, 85 (1996).

[8] V. V. Flambaum and F. M. Izrailev, Phys. Rev. E **55**, R13 (1997).

[9] V. V. Flambaum and F. M. Izrailev, Phys. Rev. E **56**, 5144 (1997).

[10] F. Borgonovi, I. Guarneri, F. M. Izrailev, and G. Casati, Report No. chao-dyn/971105 (unpublished).

[11] Y. V. Fyodorov, O. A. Chubykalo, F. M. Izrailev, and G. Casati, Phys. Rev. Lett. **76**, 1603 (1996).

[12] Numerical results are obtained within the standard numerical accuracy, that is they are independent of the integration time and of the number of chaotic trajectories.

[13] F. M. Izrailev, Phys. Rep. **196**, 299 (1990).

[14] Y. V. Fyodorov and A. D. Mirlin, Int. J. Mod. Phys. B **8**, 3795 (1994).

[15] T. Prozen and M. Robnik, J. Phys. A **23**, 1105 (1993).

[16] P. G. Silvestrov, Phys. Lett. A **209**, 173 (1995).

[17] G. Casati, V. V. Flambaum, and F. M. Izrailev (unpublished).

[18] G. Casati, B. V. Chirikov, I. Guarneri, and F. M. Izrailev, Phys. Rev. E **48**, R1613 (1993).

[19] W. Wang, F. M. Izrailev, and G. Casati, Phys. Rev. E **57**, 323 (1998).